

Long-Range Hofmeister Effects of Anionic and Cationic Amphiphiles

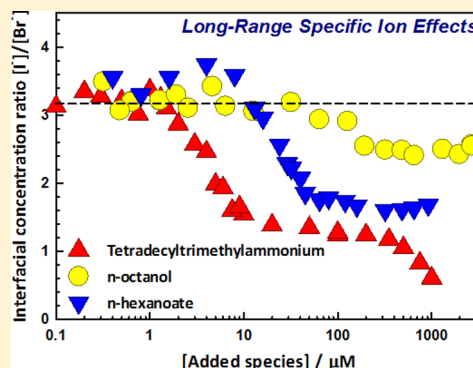
Shinichi Enami*

The Hakubi Center for Advanced Research, Kyoto University, Kyoto 606-8302, Japan
Research Institute for Sustainable Humanosphere, Kyoto University, Uji 611-0011, Japan
PRESTO, Japan Science and Technology Agency, 4-1-8 Honcho, Kawaguchi 332-0012, Japan

Agustín J. Colussi*

Ronald and Maxine Linde Center for Global Environmental Science, California Institute of Technology, California 91125, United States

ABSTRACT: Specific ion effects at aqueous interfaces play key roles in many important phenomena. We recently reported that ions interact specifically over unexpectedly long distances on the surface of sub-micromolar electrolyte solutions (Enami et al. *J. Chem. Phys.* **2012**, 136, 154707). Whether the anionic and cationic headgroups of the organic amphiphiles present at most water/hydrophobe interfaces act similarly or display new behaviors, however, is not known. Here we report the results of experiments in which we apply online electrospray ionization mass spectrometry (ESI-MS) to investigate how carboxylate, RCOO^- ($\text{R} = \text{CH}_3, \text{C}_5\text{H}_{11}, \text{C}_7\text{H}_{15}$), and alkylammonium, $\text{R}'(\text{CH}_3)_3\text{N}^+$ ($\text{R}' = \text{CH}_3, \text{C}_{14}\text{H}_{29}$), ions affect the ratio $\chi = \text{I}^-/\text{Br}^-$ at the aerial interface of 1 μM ($\text{NaI} + \text{NaBr}$) aqueous solutions. We found that χ is systematically but selectively depressed by these ionic amphiphiles and minimally affected by the neutral surfactant 1-octanol. The depressing effects induced by cationic headgroups are stronger than those caused by anionic surfactants and always increase with the length of the alkyl chains.



INTRODUCTION

Long-range specific ion effects (LR-SIEs) at water–hydrophobe (e.g., air, oil, proteins and biomembranes) interfaces control important chemical, physical, and biological phenomena.^{1–12} Natural surfactants, such as long-chain amphiphilic carboxylic acids,^{13–15} on the surface of the ocean modulate the enrichment and reactivity of anions, particularly I^- , in marine aerosols, thereby affecting the chemistry of the lower troposphere.^{13,16–24} A recent report indicated that the long-chain hexanoic and octanoic acids, in contrast with acetic acid, significantly enhance $\text{I}_2(\text{g})$ emissions from aqueous I^- solutions exposed to $\text{O}_3(\text{g})$ by supplying the requisite protons at the interface.¹⁹

Hydrophobicity plays critical roles in diverse fields, especially in vivo. Hydrophobic forces are deemed to drive the self-assembly of amphiphilic molecules into micelles and bilayers, the folding of proteins, and the fusion of biomembranes.²⁵ Their origin, however, remains controversial.^{25–27} It has been found that ions specifically affect the behaviors of hydrophobic solutes in water.²⁸ A recent experimental report showed that the presence of ions specifically alters the surface diffusivity of polymer molecules, suggesting that a perturbed interfacial region mediates the coupling of water with hydrophobic surfaces.²⁹ A simulation study revealed that the average interaction energy of solvent molecules in the surface region

is higher than that in bulk solution.³⁰ By occupying space in this region, a solute reduces the average number of solvent molecules in the interface within a distance of the Gibbs dividing surface, thereby mitigating the thermodynamic costs intrinsic to creating the phase boundary.³⁰ Recently, we found evidence that LR-SIEs operate at the surface of sub-micromolar electrolyte solutions. The inference is that ions interact specifically at separations that exceed Bjerrum lengths (i.e., the interionic separation between two monovalent ions at which their mutual electrostatic energy equals the average thermal energy, $k_{\text{B}}T$)²⁵ $\lambda_{\text{B}} = e^2/(4\pi\epsilon_0\epsilon k_{\text{B}}T) = 0.7$ or 56 nm in H_2O ($\epsilon = 78$) or vacuum ($\epsilon = 1$), respectively, in homogeneous isotropic media.³¹ This is consistent with a recent experimental study by Ninham and co-workers, who provided evidence of SIE in $<50 \mu\text{M}$ electrolytes (one ion in $>10^6$ water molecules) at a solid/water interface.²

Here we report a study on LR-SIEs induced by amphiphilic organic ions that takes advantage of the high sensitivity, surface selectivity, and unambiguous identification capabilities of online ESI-MS^{32,33} to investigate LR-SIEs in mixed (halide + carboxylate/ammonium ions) solutions films at sub-micro-

Received: February 4, 2013

Revised: April 22, 2013

Published: April 26, 2013

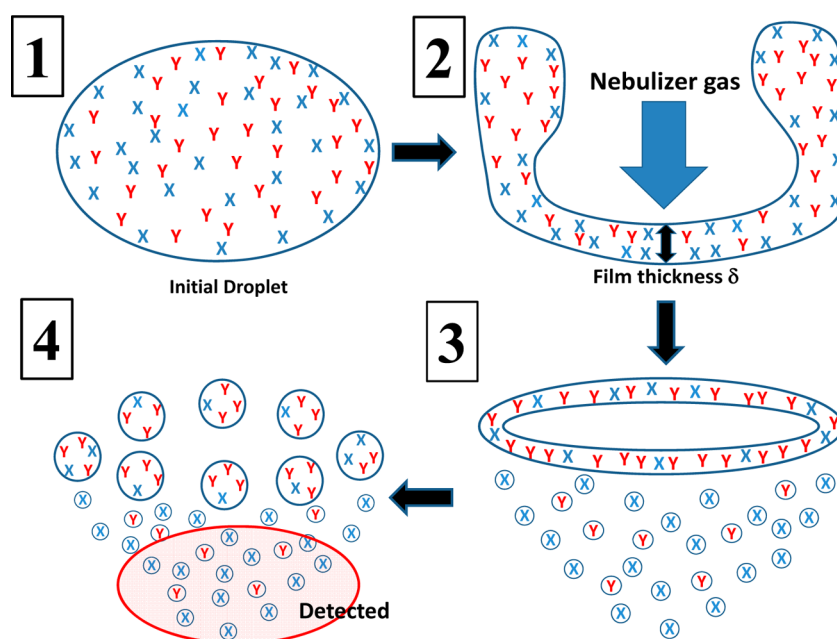


Figure 1. Schematic illustration of a droplet breakup mechanism. δ is the thickness of the film. In our experiments we detect the ions contained in the submicrometer droplets generated from the center of the film by online electrospray ionization mass spectrometry. Ions having the larger propensities for the air–liquid interface, such as I^- and $\text{C}_5\text{H}_{11}\text{COO}^-$, accumulate in the center of the film thereby producing the more intense mass signals, i.e., $[\text{X}]/[\text{Y}] > 1$. See text for details.

molar to millimolar. We have previously demonstrated that this technique is possible to selectively sample ions at the interfacial layers of liquids (see below).^{32–36} Online sampling of the surface of continually refreshed uncontaminated liquid jets under ambient temperature and pressure makes our instrument a valuable surface-sensitive technique.

EXPERIMENTAL SECTION

In our experiments we measure (in situ, via online electrospray ionization mass spectrometry, ESI-MS, Kyoto University) relative anion populations, $\chi = P_{127}/P_{79+81} = [\text{I}^-]/[\text{Br}^-]$, in the water “films” produced upon blowing up drops of sodium salt solutions by a high-speed gas as a function of cationic and anionic amphiphilic ion additions in the 0.1–1000 μM range.³¹ Here we summarize the key mechanisms that give rise to mass spectral signals. Liquid solutions (injected as jets into the spraying chamber of the mass spectrometer) are sheared into primary drops by means of a codirectional high-speed nebulizer gas.³⁷ Figure 1 shows a schematic diagram of the initial droplet breakup. These primary drops are flattened by the moving gas, and then suddenly stretched windward into rimmed thin-film bags.³⁸ Given that the proximity of dissolved ions to the air–liquid interface varies along the span of the films, ions having larger propensities for the interface (ion X in Figure 1) become naturally enriched in the thinner sections of the film.^{14,15} In this process, ions having smaller propensities (ion Y in Figure 1) accumulate in the rim whereas ions having larger propensities preferentially distribute along the film. The rimmed bags are dynamically unstable and fragment within tens of microseconds into smaller, submicrometer-sized secondary droplets.³⁹ As expected from the preceding analysis, in the case of neat water droplets, the finer droplets originating from the film are negatively charged because they contain excess anions (OH^-), whereas the coarser ones arising from the rims carry net positive charge (H^+).^{40,41} These mechanisms were experimentally confirmed by Zilch et al.⁴⁰ The enhanced surface and

electrostatic energies of the polarized stretched films are drawn from the kinetic energy of the gas. Since the kinetic energy density of the gas can deform only primary drops of $d \sim 1$ mm diameter,³⁸ the breakup of the bag into charged secondary droplets is the primordial, one-time event in which net charges (those detected by mass spectrometry) are created from the neutral inflowing solutions. Submicrometer ($d < 1 \mu\text{m}$) secondary droplets are just swept by the gas and rapidly shrink via solvent evaporation (enhanced by their large surface/volume ratios) thereby crowding their excess charges. The fact that the titration curves of carboxylic acids and trimethylammonium determined in this setup are identical with the ionization constants reported in the literature (i.e., $\text{p}K_a \sim 4.8$ and ~ 9.8 , respectively)^{32,42} suggests that solvent evaporation is minimal prior to droplet breakup. Submicrometer droplets eventually become Rayleigh-unstable and undergo a cascade of Coulomb explosions whose outcome is the ejection of bare single ions to the gas phase.^{43,44} Note that Coulomb explosions, in contrast with the aerodynamic breakup of primary droplets described above, arise from repulsion among like charges and therefore preserve the overall charges of the initial ensemble of (positively and) negatively charged secondary droplets. By electrically biasing the inlet to the detection chamber of the mass spectrometer, we can monitor ions of either charge. Gas-phase ions are then sorted out electrostatically and detected by the online mass spectrometer. Note that typical values of ion diffusion coefficients, $D \approx 2 \times 10^{-5} \text{ cm}^2 \text{ s}^{-1}$, and representative film lifetimes, $\tau \approx 10^{-5} \text{ s}$, lead to estimated mean diffusive displacements: $\lambda = (2D\tau)^{1/2} = 2 \times 10^{-5} \text{ cm}$, which are larger than the average thickness of present (nano)films, suggesting that diffusion assists ions to achieve equilibration.

We have shown that (i) the relative anion abundances at air–water interface, i.e., the mass-spectral signal intensities, measured on aqueous droplets consisting of equimolar solutions of mixed salts follow a normal Hofmeister series (as expected at the air–water interface of less than a few

nanometers thickness and confirmed by other surface-sensitive techniques) and are specifically affected by cationic or anionic surfactants,^{14,15} and (ii) mass spectra of aqueous droplets exposed to reactive gases detect species necessarily produced at the gas–liquid interface rather than in bulk water.^{34,45,46} Data analysis based on mass balances and the kinetic theory of gases¹⁶ suggest that the thickness of the interfacial layers sampled in these experiments is less than a few nanometers, most likely below 1 nm.^{32,33} More compellingly, we recently showed that the depth of the interfacial layers sampled in our experiments is controllable as a function of nebulizer gas velocity v_g .⁴⁷ This observation is consistent with the droplet breakup mechanism shown above and previous reports by other researchers.^{40,48} Under the present high v_g (~ 160 m/s) condition, ions that reside at the topmost layers of the air–water interface are preferentially detected as mass signals.⁴⁷ Further experimental details and validation tests could be found in elsewhere.^{32,36,47}

Conditions in the present experiments were as follows: drying N_2 gas flow rate, 13 L min^{-1} ; drying N_2 gas temperature, 300°C ; inlet voltage, $+3.5\text{ kV}$ relative to ground; and fragmentor voltage value, 80 V . NaI (purity $>99.5\%$), NaBr ($>99\%$), CH_3COOH ($>99.7\%$), $\text{C}_5\text{H}_{11}\text{COOH}$ ($>99\%$), $\text{C}_7\text{H}_{15}\text{COOH}$ ($>98\%$), $n\text{-C}_{14}\text{H}_{29}(\text{CH}_3)_3\text{NCl}$ ($>98\%$), $(\text{CH}_3)_4\text{NCl}$ ($>98\%$), and 1-octanol ($>98\%$) were purchased from Nacalai Tesque (Kyoto) and were used as received. All solutions were prepared in purified water (resistivity $\geq 18.2\text{ M}\Omega\text{ cm}$ at 298 K) from a Millipore Milli-Q water purification system. Carboxylic acids were pH-adjusted by concentrated NaOH solution with a calibrated pH meter (Horiba, LAQUA F-74). All experiments were performed at $298 \pm 3\text{ K}$.

RESULTS AND DISCUSSION

Figure 2 shows negative ion ESI mass spectra from aqueous equimolar $1\text{ }\mu\text{M}$ (NaI + NaBr) films in the absence/presence of RCOO^- ($\text{R} = \text{CH}_3, \text{C}_5\text{H}_{11}$) at $\text{pH} = 7.0 \pm 0.2$. In the absence of carboxylate ions, the ratio of I^- to Br^- ESI-MS signals, $\chi = P_{127}/P_{79+81}$, is ~ 3 rather than 1. On the basis of previous results and considerations, χ is ascribed to the ratio of ion populations at the air/water interface of liquid films probed by the present method (see above).^{31,47} The observation that the interfacial affinity of I^- is larger than that of Br^- is in accord with a number of independent experimental results and theoretical predictions.^{5,10,49–59} Since more than 99% of the alkylcarboxylic acids ($\text{pK}_a \sim 4.8$) are present as the conjugated carboxylate anions at $\text{pH } 7.0$, it is apparent that the net effect of carboxylate anions is to displace I^- and Br^- selectively from the interfacial layers (see below), and that $\text{C}_5\text{H}_{11}\text{COO}^-$ is significantly more effective than CH_3COO^- in this regard. Notice that $\text{C}_5\text{H}_{11}\text{COO}^-$ signal intensities are ~ 10 times larger than those of CH_3COO^- at the same concentration, revealing that, as expected, the former is more enriched than the latter at the surface.^{14,15,31} Different ions populate interfacial layers of different depths rather than a common interfacial region with different probabilities.³¹ Such rationale seems to be valid in the present case.

Figure 3, A and B, shows how the populations of I^- and Br^- at the air/water interface are affected by increasing additions of RCOO^-Na^+ ($\text{R} = \text{CH}_3, n\text{-C}_5\text{H}_{11}, n\text{-C}_7\text{H}_{15}$) or $\text{R}'(\text{CH}_3)_3\text{N}^+\text{Cl}^-$ ($\text{R}' = \text{CH}_3, n\text{-C}_{14}\text{H}_{29}$) or $1\text{-C}_8\text{H}_{17}\text{OH}$, respectively. Both I^- and Br^- signals begin to fall off upon addition of less than $\sim 10\text{ }\mu\text{M}$ carboxylate or ammonium ions in specific ways. For instance, a 10-fold depression of I^- signals requires ~ 9 times larger

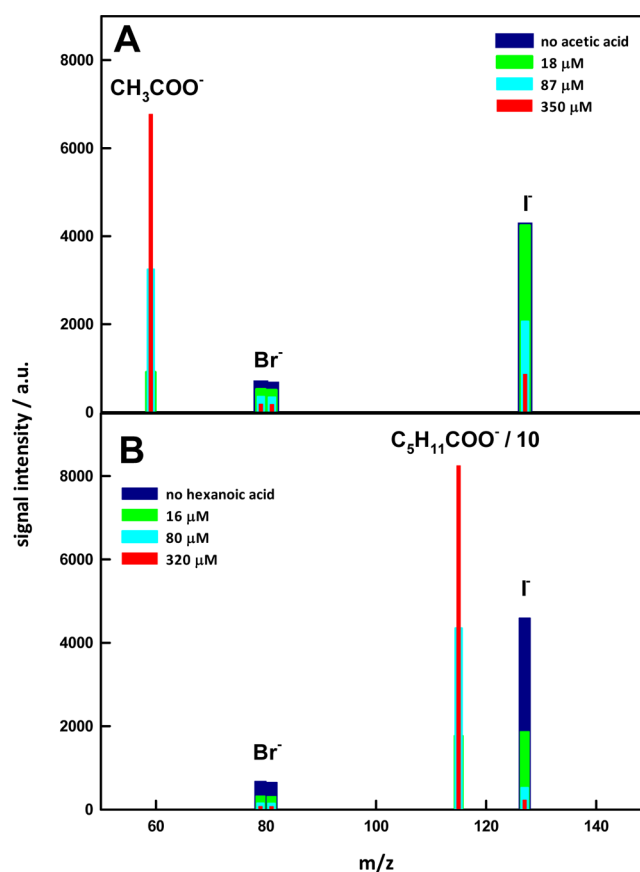


Figure 2. Negative ion ESI mass spectra from aqueous $1\text{ }\mu\text{M}$ equimolar (NaI + NaBr) solutions films in the absence/presence of acetic acid (A) and hexanoic acid (B) at $\text{pH} = 7.0 \pm 0.2$. Note that the signal intensity of $\text{C}_5\text{H}_{11}\text{COO}^-$ was divided by 10.

concentrations of added CH_3COO^- than $\text{C}_5\text{H}_{11}\text{COO}^-$ (Figure 3A). Note that in none of the experiments of Figure 3A the surface becomes saturated with carboxylates (saturation is reached at ~ 200 and $\sim 50\text{ mM}$ for acetic and hexanoic acids, respectively).^{19,60} A similar trend is observed for the alkylammonium ions (Figure 3B). In remarkable contrast, up to 3 mM additions of the neutral amphiphile 1-octanol barely affects ion signals. This result is consistent with the negligible effect of 1-octanol on the reactive uptake of gaseous trimethylamine (TMA) and NO_2 on water.^{20,36}

The existence of significant specific effects in these experiments emerges clearly from Figure 4, A and B, which displays interfacial population ratios, $\chi = P_{127}/P_{79+81}$, as functions of the concentrations of the different additives. Ostensibly, both carboxylate and alkylammonium ion additions, starting at the submicromolar range, perturb χ specifically. Note that this effect is not generic, e.g., mediated by the increased charge density of the films, but chemically specific. Ions do interact specifically at separations that exceed Bjerrum lengths.³¹ Since such exceedingly long-range interactions were also observed in a solid/water interface,² we infer LR-SIEs are universal phenomena at aqueous interfaces. R_4N^+ ions exert monotonic depressing effects throughout (Figure 4B). In contrast, carboxylate ions enhance χ below $\sim 10\text{ }\mu\text{M}$, peaking thereafter (Figure 4A). The enhancements observed at low concentrations are consistent with the competition between ions of similar interfacial affinities for the occupation of the liquid films (see above),³¹ and the fact that R-COO^-

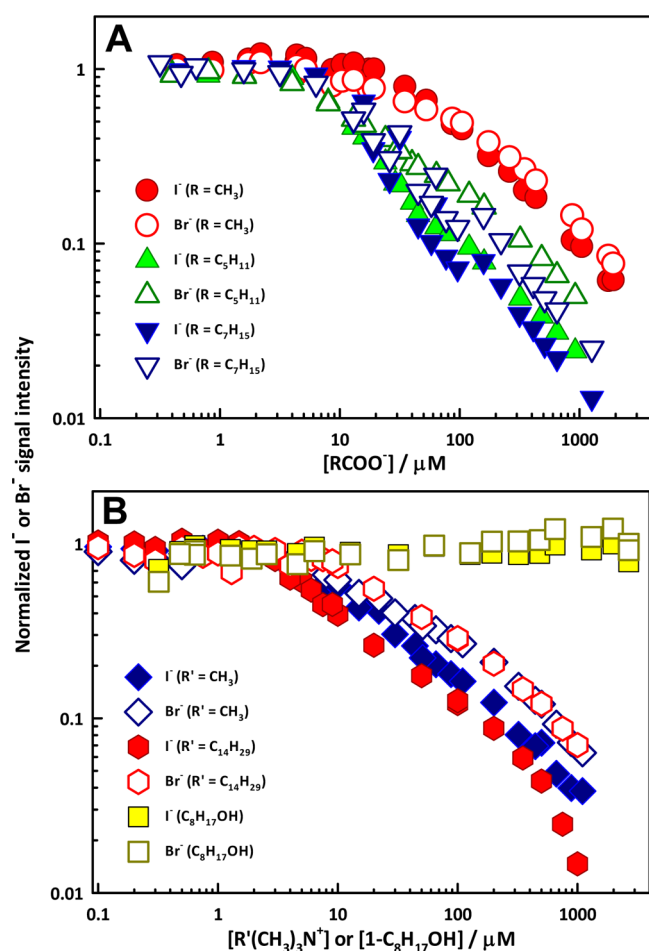


Figure 3. Log–log plots of normalized I^- or Br^- signal intensities from aqueous $1\ \mu\text{M}$ equimolar ($\text{NaI} + \text{NaBr}$) solutions films as a function of added: (A) RCOO^-Na^+ ; (B) $\text{R}'(\text{CH}_3)_3\text{N}^+\text{Cl}^-$ or 1-octanol. All experiments at $\text{pH} = 7.0 \pm 0.2$.

headgroups are expected to mainly reside in the (thicker) film sections containing Br^- , in agreement with the normal Hofmeister series, $\text{CH}_3\text{COO}^- < \text{Br}^- < \text{NO}_3^- < \text{I}^- < \text{ClO}_4^-$, and our previous results showing that ClO_4^- preferentially depresses I^- whereas NO_3^- has the opposite effect.³¹ The larger effects of the longer alkyl chain amphiphiles are consistent with their emergence to the interfacial layers at lower concentrations. All carboxylates in excess eventually populate the thinner film sections, i.e., those where I^- accumulates and which make the largest contribution to secondary droplet formation. The detectable effects of tail length in these experiments are consistent with interfacial LR-SIEs in the sub-micromolar range. The dependence on tail length of the effects of alkylammonium ions on χ must be ascribed to the direct and specific interaction of these counterions (rather than the common co-ion Cl^-) with I^- and Br^- .

In summary, we provided evidence of the existence of long-range chemically specific both co-ion and counterion effects in the outermost air–water interfacial layers. We showed that the LR-SIEs operate not only among simple inorganic ions but may also involve anionic and cationic organic amphiphiles present at most water/hydrophobe interfaces. Notably, interfacial population ratio of I^- to Br^- was minimally affected by the neutral surfactant 1-octanol. The depressing effects induced by cationic headgroups are stronger than those caused by anionic

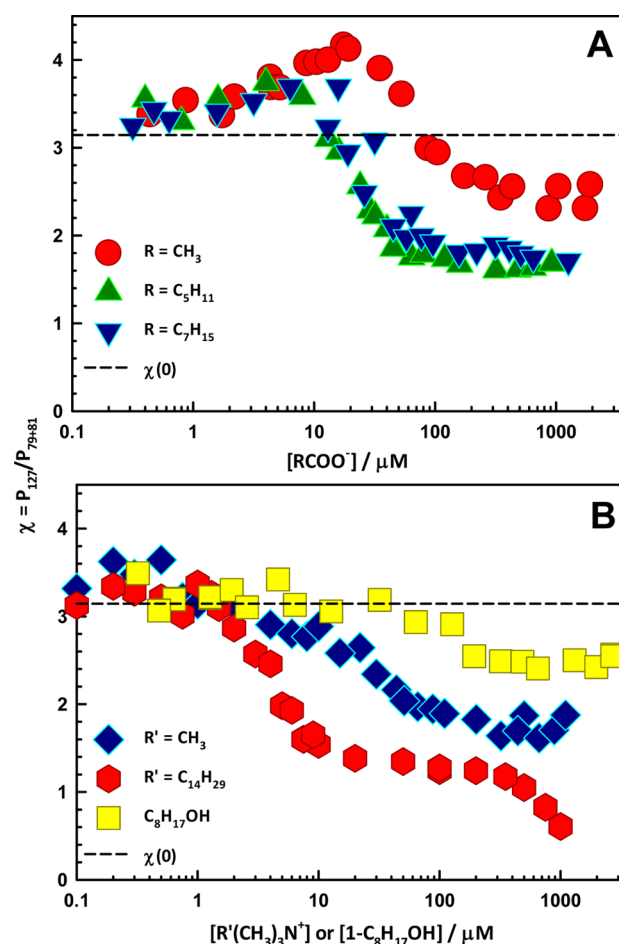


Figure 4. Semilog plots of the ESI mass spectral signal ratio $\chi = \text{I}^-/\text{Br}^-$ from aqueous $1\ \mu\text{M}$ equimolar ($\text{NaI} + \text{NaBr}$) solutions films as a function of added: (A) RCOO^-Na^+ ; (B) $\text{R}'(\text{CH}_3)_3\text{N}^+\text{Cl}^-$ or 1-octanol. All experiments at $\text{pH} = 7.0 \pm 0.2$. The dotted line corresponds to the $\chi(0)$ value measured in the absence of additives.

surfactants and increase with the length of the alkyl chains in both cases.

AUTHOR INFORMATION

Corresponding Author

*E-mail: enami.shinichi.3r@kyoto-u.ac.jp (S.E.); ajcoluss@caltech.edu (A.J.C.).

Notes

The authors declare no competing financial interest.

ACKNOWLEDGMENTS

This work was financially supported by the Japan Science and Technology Agency (JST) PRESTO program. We are grateful to Michael Hoffmann and Himanshu Mishra of Caltech for helpful discussion.

REFERENCES

- (1) Lo Nostro, P.; Ninham, B. W. Hofmeister Phenomena: An Update on Ion Specificity in Biology. *Chem. Rev.* **2012**, *112*, 2286–2322.
- (2) Borah, J. M.; Mahiuddin, S.; Sarma, N.; Parsons, D. F.; Ninham, B. W. Specific Ion Effects on Adsorption at the Solid/Electrolyte Interface: A Probe into the Concentration Limit. *Langmuir* **2011**, *27*, 8710–8717.

- (3) Kunz, W.; Lo Nostro, P.; Ninham, B. W. The Present State of Affairs with Hofmeister Effects. *Curr. Opin. Colloid Interface Sci.* **2004**, *9*, 1–18.
- (4) Pegram, L. M.; Wendorff, T.; Erdmann, R.; Shkel, I.; Bellissimo, D.; Felitsky, D. J.; Record, M. T. Why Hofmeister Effects of Many Salts Favor Protein Folding but Not DNA Helix Formation. *Proc. Natl. Acad. Sci. U.S.A.* **2010**, *107*, 7716–7721.
- (5) Jungwirth, P.; Tobias, D. J. Specific Ion Effects at the Air/Water Interface. *Chem. Rev.* **2006**, *106*, 1259–1281.
- (6) Parsons, D. F.; Bostrom, M.; Lo Nostro, P.; Ninham, B. W. Hofmeister Effects: Interplay of Hydration, Nonelectrostatic Potentials, and Ion Size. *Phys. Chem. Chem. Phys.* **2011**, *13*, 12352–12367.
- (7) Schelero, N.; von Klitzing, R. Correlation between Specific Ion Adsorption at the Air/Water Interface and Long-Range Interactions in Colloidal Systems. *Soft Matter* **2011**, *7*, 2936–2942.
- (8) Petersen, P. B.; Saykally, R. J. On the Nature of Ions at the Liquid Water Surface. *Annu. Rev. Phys. Chem.* **2006**, *57*, 333–364.
- (9) Rankin, B. M.; Hands, M. D.; Wilcox, D. S.; Fega, K. R.; Slipchenko, L. V.; Ben-Amotz, D. Interactions between Halide Anions and a Molecular Hydrophobic Interface. *Faraday Discuss.* **2013**, *160*, 255–270.
- (10) Marcus, Y. Individual Ionic Surface Tension Increments in Aqueous Solutions. *Langmuir* **2013**, *29*, 2881–2888.
- (11) Stern, A. C.; Baer, M. D.; Mundy, C. J.; Tobias, D. J. Thermodynamics of Iodide Adsorption at the Instantaneous Air-Water Interface. *J. Chem. Phys.* **2013**, *138*, 114709.
- (12) Friedman, R. Ions and the Protein Surface Revisited: Extensive Molecular Dynamics Simulations and Analysis of Protein Structures in Alkali-Chloride Solutions. *J. Phys. Chem. B* **2011**, *115*, 9213–9223.
- (13) Enami, S.; Vecitis, C. D.; Cheng, J.; Hoffmann, M. R.; Colussi, A. J. Global Inorganic Source of Atmospheric Bromine. *J. Phys. Chem. A* **2007**, *111*, 8749–8752.
- (14) Cheng, J.; Vecitis, C.; Hoffmann, M. R.; Colussi, A. J. Experimental Anions Affinities for the Air/Water Interface. *J. Phys. Chem. B* **2006**, *110*, 25598.
- (15) Cheng, J.; Hoffmann, M. R.; Colussi, A. J. Anion Fractionation and Reactivity at Air/Water:Methanol Interfaces. Implications for the Origin of Hofmeister Effects. *J. Phys. Chem. B* **2008**, *112*, 7157.
- (16) Davidovits, P.; Kolb, C. E.; Williams, L. R.; Jayne, J. T.; Worsnop, D. R. Mass Accommodation and Chemical Reactions at Gas-Liquid Interfaces. *Chem. Rev.* **2006**, *106*, 1323–1354.
- (17) Finlayson-Pitts, B. J. Reactions at Surfaces in the Atmosphere: Integration of Experiments and Theory as Necessary (but Not Necessarily Sufficient) for Predicting the Physical Chemistry of Aerosols. *Phys. Chem. Chem. Phys.* **2009**, *11*, 7760–7779.
- (18) Donaldson, D. J.; Valsaraj, K. T. Adsorption and Reaction of Trace Gas-Phase Organic Compounds on Atmospheric Water Film Surfaces: A Critical Review. *Environ. Sci. Technol.* **2010**, *44*, 865–873.
- (19) Hayase, S.; Yabushita, A.; Kawasaki, M.; Enami, S.; Hoffmann, M. R.; Colussi, A. J. Weak Acids Enhance Halogen Activation on Atmospheric Water's Surfaces. *J. Phys. Chem. A* **2011**, *115*, 4935–4940.
- (20) Kinugawa, T.; Enami, S.; Yabushita, A.; Kawasaki, M.; Hoffmann, M. R.; Colussi, A. J. Conversion of Gaseous Nitrogen Dioxide to Nitrate and Nitrite on Aqueous Surfactants. *Phys. Chem. Chem. Phys.* **2011**, *13*, 5144–5149.
- (21) Brown, M. A.; Ashby, P. D.; Ogletree, D. F.; Salmeron, M.; Hemminger, J. C. Reactivity of Ozone with Solid Potassium Iodide Investigated by Atomic Force Microscopy. *J. Phys. Chem. C* **2008**, *112*, 8110–8113.
- (22) Ghosal, S.; Brown, M. A.; Bluhm, H.; Krisch, M. J.; Salmeron, M.; Jungwirth, P.; Hemminger, J. C. Ion Partitioning at the Liquid/Vapor Interface of a Multicomponent Alkali Halide Solution: A Model for Aqueous Sea Salt Aerosols. *J. Phys. Chem. A* **2008**, *112*, 12378–12384.
- (23) Rouviere, A.; Ammann, M. The Effect of Fatty Acid Surfactants on the Uptake of Ozone to Aqueous Halogenide Particles. *Atmos. Chem. Phys.* **2010**, *10*, 11489–11500.
- (24) Krisch, M. J.; D'Auria, R.; Brown, M. A.; Tobias, D. J.; Hemminger, J. C.; Ammann, M.; Starr, D. E.; Bluhm, H. The Effect of an Organic Surfactant on the Liquid-Vapor Interface of an Electrolyte Solution. *J. Phys. Chem. C* **2007**, *111*, 13497–13509.
- (25) Israelachvili, J. *Intermolecular & Surface Forces*, 3rd ed.; Academic Press: London, 2011.
- (26) Godec, A.; Merzel, F. Physical Origin Underlying the Entropy Loss Upon Hydrophobic Hydration. *J. Am. Chem. Soc.* **2012**, *134*, 17574–17581.
- (27) Davis, J. G.; Gierszal, K. P.; Wang, P.; Ben-Amotz, D. Water Structural Transformation at Molecular Hydrophobic Interfaces. *Nature* **2012**, *491*, 582–585.
- (28) Holz, M.; Grunder, R.; Sacco, A.; Meleleo, A. Nuclear-Magnetic-Resonance Study of Self-Association of Small Hydrophobic Solutes in Water - Salt Effects and the Lyotropic Series. *J. Chem. Soc., Faraday Trans.* **1993**, *89*, 1215–1222.
- (29) Yang, Q. B.; Zhao, J. Hofmeister Effect on the Interfacial Dynamics of Single Polymer Molecules. *Langmuir* **2011**, *27*, 11757–11760.
- (30) Otten, D. E.; Shaffer, P. R.; Geissler, P. L.; Saykally, R. J. Elucidating the Mechanism of Selective Ion Adsorption to the Liquid Water Surface. *Proc. Natl. Acad. Sci. U.S.A.* **2012**, *109*, 701–705.
- (31) Enami, S.; Mishra, H.; Hoffmann, M. R.; Colussi, A. J. Hofmeister Effects in Micromolar Electrolyte Solutions. *J. Chem. Phys.* **2012**, *136*, 154707.
- (32) Enami, S.; Hoffmann, M. R.; Colussi, A. J. Proton Availability at the Air/Water Interface. *J. Phys. Chem. Lett.* **2010**, *1*, 1599–1604.
- (33) Enami, S.; Stewart, L. A.; Hoffmann, M. R.; Colussi, A. J. Superacid Chemistry on Mildly Acidic Water. *J. Phys. Chem. Lett.* **2010**, *1*, 3488–3493.
- (34) Enami, S.; Hoffmann, M. R.; Colussi, A. J. Acidity Enhances the Formation of a Persistent Ozonide at Aqueous Ascorbate/Ozone Gas Interfaces. *Proc. Natl. Acad. Sci. U.S.A.* **2008**, *105*, 7365–7369.
- (35) Enami, S.; Hoffmann, M. R.; Colussi, A. J. Prompt Formation of Organic Acids in Pulse Ozonation of Terpenes on Aqueous Surfaces. *J. Phys. Chem. Lett.* **2010**, *1*, 2374–2379.
- (36) Enami, S.; Hoffmann, M. R.; Colussi, A. J. Molecular Control of Reactive Gas Uptake “on Water”. *J. Phys. Chem. A* **2010**, *114*, 5817–5822.
- (37) Marmottant, P. H.; Villermaux, E. On Spray Formation. *J. Fluid Mech.* **2004**, *498*, 73–111.
- (38) Theofanous, T. G.; Mitkin, V. V.; Ng, C. L.; Chang, C. H.; Deng, X.; Sushchikh, S. The Physics of Aerobreakup. II. Viscous Liquids. *Phys. Fluids* **2012**, *24*, 022104.
- (39) Pilch, M.; Erdman, C. A. Use of Breakup Time Data and Velocity History Data to Predict the Maximum Size of Stable Fragments for Acceleration-Induced Breakup of a Liquid-Drop. *Int. J. Multiphase Flow* **1987**, *13*, 741–757.
- (40) Zilch, L. W.; Maze, J. T.; Smith, J. W.; Ewing, G. E.; Jarrold, M. F. Charge Separation in the Aerodynamic Breakup of Micrometer-Sized Water Droplets. *J. Phys. Chem. A* **2008**, *112*, 13352–13363.
- (41) Bhattacharyya, I.; Maze, J. T.; Ewing, G. E.; Jarrold, M. F. Charge Separation from the Bursting of Bubbles on Water. *J. Phys. Chem. A* **2011**, *115*, 5723–5728.
- (42) Mishra, H.; Enami, S.; Nielsen, R. J.; Stewart, L. A.; Hoffmann, M. R.; Goddard, W. A.; Colussi, A. J. Brønsted Basicity of the Air-Water Interface. *Proc. Natl. Acad. Sci. U.S.A.* **2012**, *109*, 18679–18683.
- (43) Iribarne, J. V.; Thomson, B. A. On the Evaporation of Small Ions from Charged Droplets. *J. Chem. Phys.* **1976**, *64*, 2287.
- (44) Nguyen, S.; Fenn, J. B. Gas-Phase Ions of Solute Species from Charged Droplets of Solutions. *Proc. Natl. Acad. Sci. U.S.A.* **2007**, *104*, 1111–1117.
- (45) Enami, S.; Hoffmann, M. R.; Colussi, A. J. Dry Deposition of Biogenic Terpenes Via Cationic Oligomerization on Environmental Aqueous Surfaces. *J. Phys. Chem. Lett.* **2012**, *3*, 3102–3108.
- (46) Enami, S.; Vecitis, C. D.; Cheng, J.; Hoffmann, M. R.; Colussi, A. J. Electrospray Mass Spectrometric Detection of Products and Short-Lived Intermediates in Aqueous Aerosol Microdroplets Exposed to a Reactive Gas. *J. Phys. Chem. A* **2007**, *111*, 13032–13037.

- (47) Enami, S.; Colussi, A. J. Long-Range Specific Ion-Ion Interactions in Hydrogen-Bonded Liquid Films. *J. Chem. Phys.* **2013**, in press.
- (48) Rimbart, N.; Castanet, G. Crossover between Rayleigh-Taylor Instability and Turbulent Cascading Atomization Mechanism in the Bag-Breakup Regime. *Phys. Rev. E* **2011**, *84*, 016318.
- (49) Petersen, P. B.; Saykally, R. J. Confirmation of Enhanced Anion Concentration at the Liquid Water Surface. *Chem. Phys. Lett.* **2004**, *397*, 51.
- (50) Petersen, P. B.; Saykally, R. J. Adsorption of Ions to the Surface of Dilute Electrolyte Solutions: The Jones-Ray Effect Revisited. *J. Am. Chem. Soc.* **2005**, *127*, 15446–15452.
- (51) Ottosson, N.; Cwiklik, L.; Soderstrom, J.; Bjorneholm, O.; Ohrwall, G.; Jungwirth, P. Increased Propensity of I(Aq)(-) for the Water Surface in Non-Neutral Solutions: Implications for the Interfacial Behavior of H(3)O(Aq)(+) and OH(Aq)(-). *J. Phys. Chem. Lett.* **2011**, *2*, 972–976.
- (52) Baer, M. D.; Mundy, C. J. Toward an Understanding of the Specific Ion Effect Using Density Functional Theory. *J. Phys. Chem. Lett.* **2011**, *2*, 1088–1093.
- (53) Pegram, L. M.; Record, M. T. Partitioning of Atmospherically Relevant Ions between Bulk Water and the Water/Vapor Interface. *Proc. Natl. Acad. Sci. U.S.A.* **2006**, *103*, 14278–14281.
- (54) Netz, R. R.; Horinek, D. Progress in Modeling of Ion Effects at the Vapor/Water Interface. *Annu. Rev. Phys. Chem.* **2012**, *63*, 401–418.
- (55) Kalcher, L.; Horinek, D.; Netz, R. R.; Dzubiella, J. Ion Specific Correlations in Bulk and at Biointerfaces. *J. Phys.: Condens. Matter* **2009**, *21*, 424108.
- (56) Horinek, D.; Herz, A.; Vrbka, L.; Sedlmeier, F.; Mamatkulov, S. I.; Netz, R. R. Specific Ion Adsorption at the Air/Water Interface: The Role of Hydrophobic Solvation. *Chem. Phys. Lett.* **2009**, *479*, 173–183.
- (57) Tian, C. S.; Byrnes, S. J.; Han, H. L.; Shen, Y. R. Surface Propensities of Atmospherically Relevant Ions in Salt Solutions Revealed by Phase-Sensitive Sum Frequency Vibrational Spectroscopy. *J. Phys. Chem. Lett.* **2011**, *2*, 1946–1949.
- (58) Ghosal, S.; Hemminger, J. C.; Bluhm, H.; Mun, B. S.; Hebenstreit, E. L. D.; Ketteler, G.; Ogletree, D. F.; Requejo, F. G.; Salmeron, M. Electron Spectroscopy of Aqueous Solution Interfaces Reveals Surface Enhancement of Halides. *Science* **2005**, *308*, 563–566.
- (59) Verreault, D.; Hua, W.; Allen, H. C. From Conventional to Phase-Sensitive Vibrational Sum Frequency Generation Spectroscopy: Probing Water Organization at Aqueous Interfaces. *J. Phys. Chem. Lett.* **2012**, *3*, 3012–3028.
- (60) *CRC Handbook of Chemistry and Physics*, 90th ed.; CRC Press: Boca Raton, FL, 2009.